Journal of the Civil Engineering Forum, September 2024, 10(3):249-256
DOI 10.22146/jcef.13020
Available Online at https://jurnal.ugm.ac.id/v3/jcef/issue/archive

Proposal and Evaluation of Vertical Vibration Theory of Air Caster

Tetsunoshin Ito[1], Mehrdad Sadeghzadeh Nazari[2,*], Kazuaki Inaba[3]
[1]Graduate student, Tokyo Institute of Technology, Tokyo, JAPAN
[2]Associate Professor (Lecturer), Tokyo Institute of Technology, Tokyo, JAPAN
[3]Professor, Tokyo Institute of Technology, Tokyo, JAPAN
*Corresponding author: mehrdad.aa@m.titech.ac.jp

SUBMITTED 23 April 2024 **REVISED** 19 June 2024 **ACCEPTED** 03 July 2024

ABSTRACT Urbanization and human development have increased the exposure of seismic risk. Therefore, engineers need to develop new and more efficient technologies to protect people and objects from the disastrous consequences of earthquakes. Air casters have gained attention and have been utilized in the past decade as effective seismic vibration control devices. Although such active isolation systems perform well in mitigating horizontal input vibrations, they might cause excessive rocking motions, if not designed properly. This fact emphasizes the importance of exploring the vertical dynamic properties of air isolation systems. To gain such an understanding, this research examines and proposes a formula for the vertical stiffness and damping of air caster systems. Theoretical solutions to the vertical stiffness and damping of such systems have been explored. Computer simulations considering fluid-structure interaction have also been performed to understand the dynamic behavior of the supporting air layer. Results have been compared to validate the proposed dynamic quantities within the considered simulation range. It is also concluded that the instantaneous air layer thickness, representing the air chamber pressure, and the bearing inlet flow rate are the key factors in determining the dynamic properties of the air layer. It is concluded that to evaluate the performance of the air caster seismic isolation device and increase the probability that the qualified seismic isolation performance will be exhibited, it is necessary to investigate which parameters are greatly involved in the viscous damping coefficient and the spring constant of a mass-spring-damper system equivalent to the air caster isolation system.

KEYWORDS Air Caster; Earthquake; Stiffness; Viscous Damping Coefficient; Seismic Isolation

1 INTRODUCTION

The expansion of urban areas and advancements in population development are increasing the exposure factors of earthquake risk. To counter the increased risk, researchers need to innovate and devise advanced technologies that are more effective in safeguarding individuals and structures from the devastating impact of seismic events. Ai caster seismic isolation is one of such innovative control strategies that has gained attention in recent years.

Seismic control devices, in general, provide seismic resistance to protect structures against earthquakes through active control and passive control. When it comes to passive technologies, most of the research that has been done so far has been on materials that can withstand earthquakes, or structures that make full use of them. Examples of past research include experimental research on polymer cement mortar, research on high-performance cement-based composite materials (Suwada et al., 2005), and experimental research on reinforcement of SRC structures (Ito et al., 2013). The advantage of these technologies is that they do not require external power to operate (Ishiyama, 1992). Therefore, there is no risk of the system failing to provide seismic isolation performance. On the other hand, active seismic isolation devices have been attracting attention in recent years. They are devices that avoid earthquake motion by applying energy from the outside and activating a control system (Aoki et al., 2015).

Some active control systems, on the other hand, switch control methods depending on the transmitted seismic motion to provide optimal seismic isolation performance, while others have a structure in which the seismic isolation target object itself moves depending on the transmitted seismic motion to protect itself. The advantage of this control method is that it can always provide optimal seismic isolation as per the control system's requirements. Since seismic motion has a complex waveform, active control is effective in that it can flexibly respond to it (Adachi and Takahara, 2022).

Air casters are innovative devices that are mainly used inis lifting and moving heavy objects and machinery (SN-Engineering Inc., 2024). An air caster seismic isolation device is a device that can actively protect a structure from earthquake motion (Furuya et al., 2020), unlike earthquake-resistant designs that use vibration-resistant materials. The mechanism by which this seismic isolation device works is explained below. First,

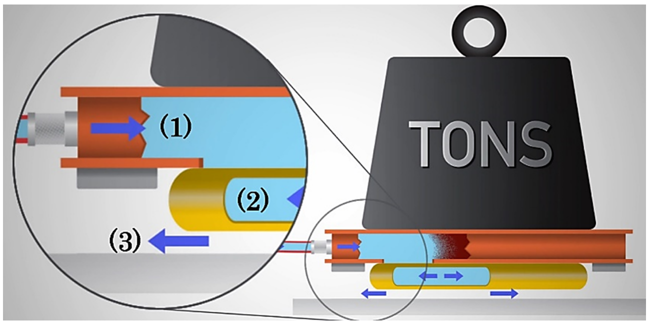

Figure 1 Performance of a seismic air isolation device (AreGo Inc., 2024) : (1) Accelerometer detects the ground shaking, (2) Air supplies from the air compressor, and (3) An air layer is created between the ground and the object

the accelerometer detects the ground motion. It is also conceivable that it will be operated by an earthquake early warning. Then, by the means of a compressor, air flows into the device. The air flowing into the device is blown towards the ground. Eventually, the air blown on the ground causes the seismic isolation device and the objects on it to leave the ground and float. By creating a layer of air between the ground and the equipment, it is possible to create a situation where the ground motion does not propagate to the objects above (Sansei Air Danshin System Inc., 2024). This device creates an air layer between the ground and the levitating object, blocking vibration (Onoda Sngyo Inc., 2024). This mechanism is illustrated in Figure 1.

While base isolation techniques have been widely used around the world, a key challenge in base-isolated structures is their susceptibility to long-period and far-field base excitations. Combining base isolation with other control, such as Tuned Mass Damper (TMD) systems, could improve the control effectiveness and overall structural performance, particularly in the case of air-base-isolated structures with significantly long natural periods. There are various types of TMDs utilized in buildings and other structures to mitigate undesired excitations. Novel TMDs, such as the passive Tuned Roller Mass Damper (TRMD), could be used in combination with air isolation systems to provide additional damping and restoring force (Sadeghzadeh Nazari et al., 2015).

Another key aspect in seismic isolation is the consideration of all the six degrees of ground motions, including translational and rotational (rocking and torsional) components. In an air caster isolation system, translational and torsional ground excitations are countered by the lateral shearing resistances in between the layers of pressurized air. Accordingly, due to the relatively low viscosity of the air, air isolation systems perform pretty well in isolating such base excitation components (Fujita et al., 2011). However, the earthquake rocking components can lead to excessive responses, overturning, or instability of the isolated structure, if not accounted for. In addition to the rocking component inherent in the ground excitation, rocking motion in a controlled structure may also occur when the horizontal center of mass and the vertical center of stiffness of the structure do not align on a vertical line. In such cases, even vertical ground motion components alone could cause rocking of the controlled structure (Furuya et al., 2020). For either reason, the presence of a rocking components emphasizes the importance of exploring the vertical dynamic properties of air isolation systems. That is because any rocking motion is supposed to be countered by the vertical stiffness and damping of the air layer supporting the controlled structure. To gain such an understanding, this paper focuses on the vertical stiffness and damping of air caster systems. Such information would be crucial in appropriate design of air isolation systems in order to limit any undesired vertical displacements.

Here, it should be pointed out that while in some practical applications pressurized air covers the whole surface of the isolated base (Sansei Air Danshin System Inc., 2024) in many other applications, a number of air isolator units are installed only in the outer corners of the base, just enough to provide structural stability. As an advantage to the latter cases, each unit would operate separately, and thus, simultaneous pressure increases and decrease due to rocking would not occur in a single unit (Furuya et al., 2020).

It is also noteworthy that although appropriately controlling the air layer stiffness and damping would be the main step in preventing excessive displacements in air isolation systems, there are also additional secondary safety measures in place for extreme scenarios. These may include elastomers and interlocking mechanisms to, respectively, resist any excessive compressive and tensile/shearing displacements (Sansei Air Danshin System Inc., 2024).

While air base isolators can be utilized for the seismic control of objects and structures on the ground, they could also be adapted to isolate non-structural elements installed on structural floors. Floor response amplification, as compared to ground excitation, emphasizes the importance of implementing appropriate design and control strategies for non-structural components (Sadeghzadeh Nazari and Ghafory Ashtiany, 2011). One effective technique for the control of non-structural elements involves using air base isolation. However, further studies, including floor spectral response analyses, are needed to ensure any excessive responses due to period elongation caused by such techniques are avoided.

A noteworthy part of an air-base-isolation system is the air layer, as it contains high-speed fluid to levitate heavy objects, and therefore requires consideration of compressible fluid. When considering horizontal vibration in this device, since it is a turbulent flow between flat plates in the high Reynolds number range, it is necessary to consider the turbulent boundary layer (Bird et al., 2018) and the frictional resistance that the fluid exerts on the levitating object against the fluid flowing through the air layer (Mitsuishi et al., 2021). Although research on air isolation as a seismic control device has been limited, pressurized air in the form of air bearings has contributed to many mechanical applications such as those in high-speed rotary nozzle flapper systems (Xu et al., 2023).

When analyzing the behavior of air-base-isolation systems, it is essential to take into account the interaction between the dynamic responses of the supporting air layer and the controlled structure responses. As the response of the controlled structure changes over time, it causes the air layer dynamic properties also to change. In other words, while the air layer affects the structural responses, the responses, in return, affect the air layer damping and stiffness. This fact emphasizes that it is essential to take into account the fluidstructure interaction effects for such analyses (You and Inaba, 2013). Another challenging aspect of the air isolation phenomenon is the need to consider cavitation effects on the solid interface between the air layer and the ground, as well as that between the air layer and the controlled structure. Considering the fluid flow pressure variations throughout the isolation procedure, cavitation would be a crucial factor for ensuring the desired functionality of the air isolation system during its service life (Kojima et al., 2018).

The air caster device is innovative in that it can separate objects from the ground (Fujita et al., 2011). However, at present, there is no established method for evaluating the performance of this device. Therefore, it is not known how this device behaves when activated. There is a possibility that a large vertical vibration will occur when levitating, or that the device may not levitate. Due to the nature of this device, if it fails to float, it will be directly hit by earthquake motion. This study focuses on the vertical vibration of this device. This device floats when an earthquake occurs, so vertical vibration plays a very important role for this device. This research will contribute to the normal functioning of the air caster seismic isolation system by proposing theoretical formulas for the viscous damping coefficient and spring constant for evaluating the performance of air casters, and verifying them by simulation. It also makes it possible to consider the performance of the seismic isolation device when designing it.

2 METHODOLOGY

2.1 Theoretical formula

Various parameters are influential in the performance of air casters, for example, the air layer pressure, air layer thickness, etc. An air caster seismic isolation device is shown in Figure 2. The vertical vibration of air casters can be expressed using the following simple dynamic model. When an air caster vibrates vertically, there should be a spring constant and a viscous damping coefficient, just like normal vibrations. First, these two theoretical formulae are proposed.

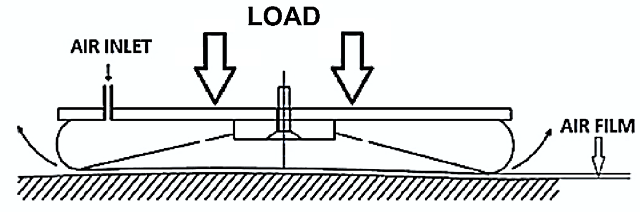

Figure 2 Simplified view of the air caster (Furuya et al., 2020)

As Figure 3 illustrates, the air caster system is equivalated to a simplified mass-spring-damper system. Since this study focuses on the vertical dynamic characteristics of the air caster, horizontal stiffnesses or damping are not described in this paper and are not shown in Figure 3.

The theoretical formulas are those of an air damper. An air damper is a device that dampens vibrations using damping force generated from air pressure. It is similar to air casters in that air is involved in the vibration. A simplified diagram of the air damper is shown in Figure 4, in which similarities with an air caster can be seen.

2.2 Proposal of the theoretical formula

Based on the mechanism explained in section 2.1, it is proposed to use the formula of air dampers for the vertical stiffness and damping of air caster isolation systems. So, the air damper design equations proposed as theoretical equations in this research are the following formula suggested by Asami (1994) :

$$k = \frac{\gamma p_0 A_p}{h_p} \frac{N^2}{1+N^2} \tag{1}$$

$$c = \frac{\gamma p_0 A_p}{\omega h_p} \frac{N^2}{1+N^2} \tag{2}$$

$$N = \sqrt{\frac{1}{2}(\sqrt{1+N_1^4}-1)} \tag{3}$$

$$N_1 = \frac{\omega A_p h_p}{\gamma p_0} \tag{4}$$

$$\alpha_1 = \frac{\sqrt{\gamma p_0 \rho_0 y_0 / h_p}}{b_1(c_0 A_0 + c_d A_d} \tag{5}$$

where, b_1 is a constant (1.112835789), c_0 and c_d are the flow coefficients, A_0 and A_d are the inlet and outlet areas, d_p is the diameter of the levitating object, A_p is the

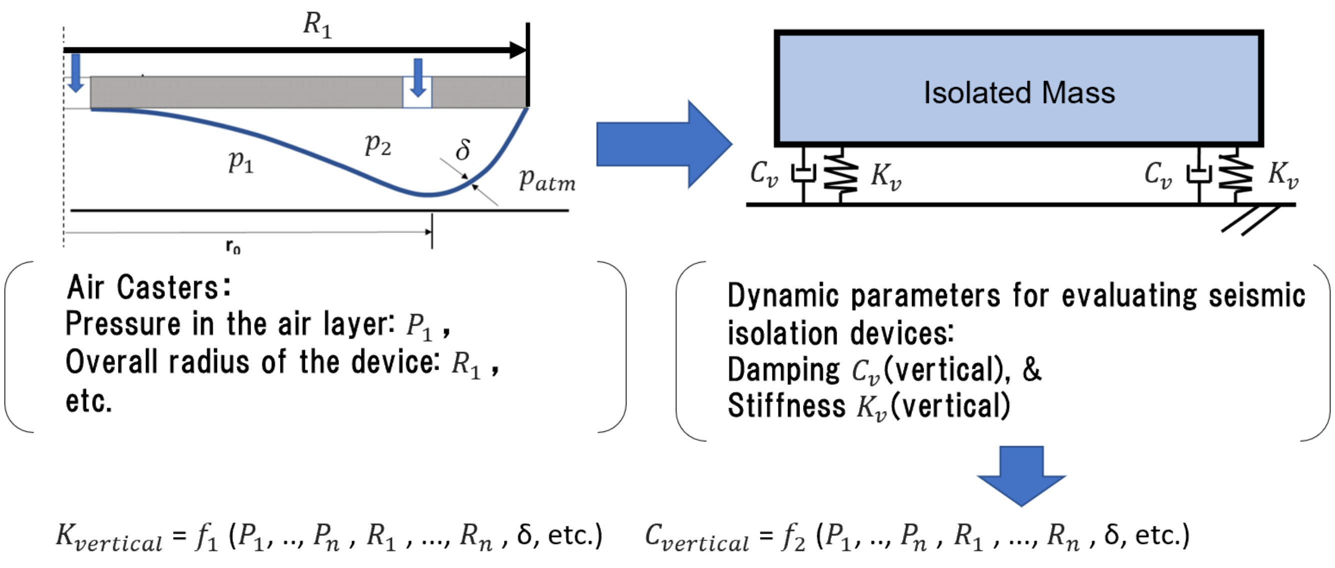

Figure 3 How to evaluate the performance of air casters (Furuya et al., 2020)

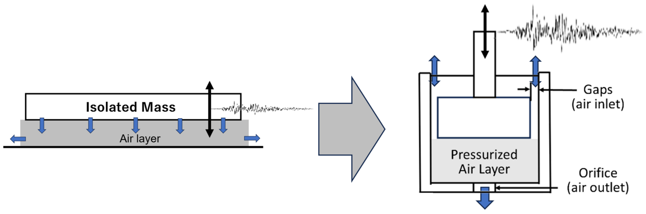

Figure 4 Similarity between air casters and air dampers: (left) inlet is from the bottom of the object; outlet is between the object and the ground, (right) inlet is the piston-cylinder gap; outlet is the orifice

base area of the levitating object, h_p is the height from the ground to the base of a levitating object, ρ_o is the density of the atmosphere, p_o is atmospheric pressure, and γ is the specific heat ratio of air (=1.4).

These are complex equations, but it can be seen that various parameters are involved in performance. The same is true for simulations, but K and C are changing from moment to moment because the influence of air on vibrating objects changes as the pressure and height of the air layer change.

2.3 Simulation

A computer simulation was performed to measure the vertical behavior of a floating object using the finite element analysis software ANSYS Fluent 2020. Figure 5 shows the geometry and details of the air caster finite element simulation model: part (a) shows the mesh for this simulation, and part (b) shows the simulation pressure distribution. Table 1 shows the initial conditions of the simulation. The vertical vibration displacement was measured from the simulation, and K and C were derived from it.

Table 1. Initial Conditions for Simulation

Parameter	Value
Mass (kg)	10
Inlet air velocity (m/s)	0.3
In-plane dimension of isolated mass (mm)	360
Initial air layer thickness (mm)	10

3 RESULTS

3.1 Simulation

The graph in Figure 6 illustrates the results of a vertical free vibration FEM simulation conducted under the initial conditions outlined in Table 1. The graph depicts the changes in the relative displacement of a 10 kg isolated mass, with the ground remaining stationary and without shaking. The mass is initially released from a height of 10 centimeters above the ground with a velocity of zero, while pressurized air flows underneath it at an inlet air velocity of 0.3 m s^{-1}. It should be noted that since the purpose of this simulation is to understand the vertical natural dynamic characteristics (K and C) of the compressed air layer, no ground excitation is applied.

Until up to 50 milliseconds, it is considered to be free fall or not sufficiently affected by the air layer. After 300 milliseconds, the vibration subsides, and it can be seen that the height is somewhat constant. From the vibration graph above, the maximum and minimum values can be observed. When the period between the two maximums and the two minimums was measured, it was found that they were not constant. In other words, it is considered necessary to use some method to produce instantaneous K and C. Figure 7 shows the vertical vibration displacement, velocity, and acceleration graphs.

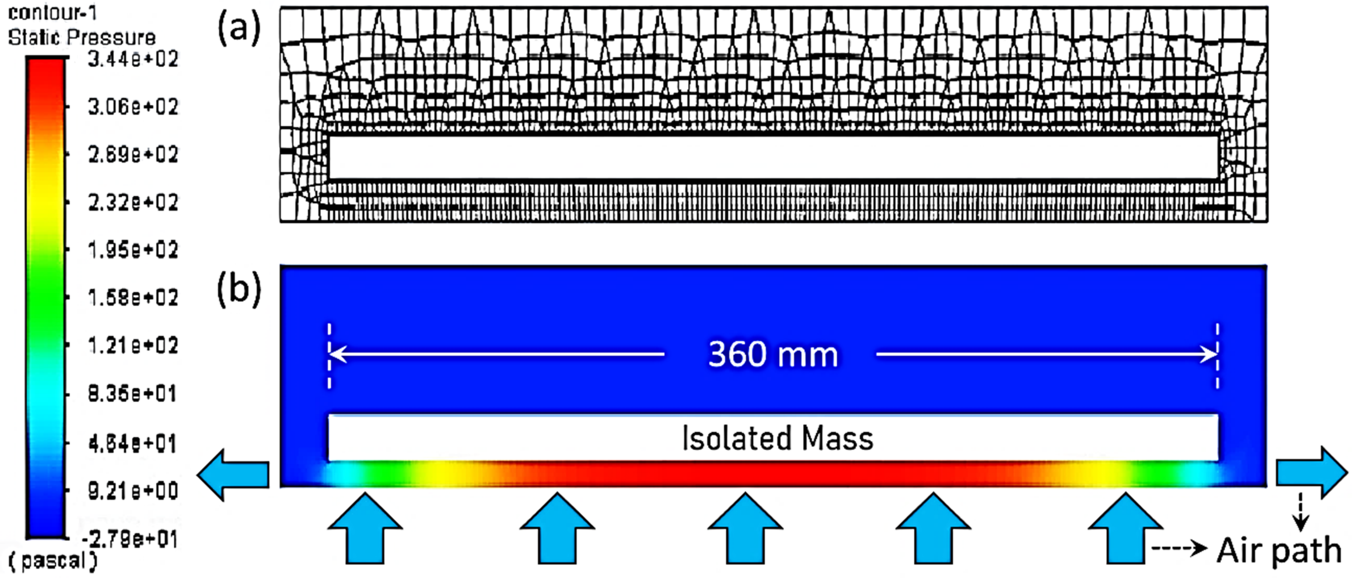

Figure 5 Geometry and details of the air casters finite element simulation in ANSYS Fluent 2020

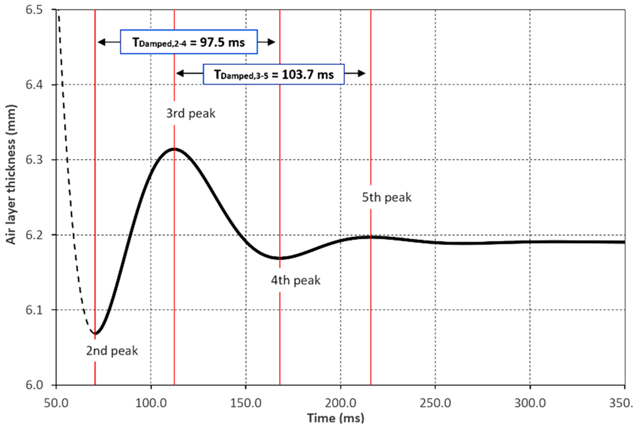

Figure 6 Vertical vibration displacement of levitating objects based on the FEM simulation

It should be noted that, in general, a higher frequency content in acceleration time history compared to displacement and velocity can be attributed to the nature of the physical phenomena being studied. In many scenarios, acceleration tends to emphasize high-frequency components, capturing rapid and transient variations in motion. In such scenarios, velocity - that assigns equal importance to high and low frequency components and displacement that represents the actual position of an object typically exhibit lower frequency behaviors. However, in other scenarios such as the free vibration modeled in Figure 7, the motion consists of smooth, gradual accelerations and decelerations. This means the free vibration motion of the isolated mass, involves relatively gradual changes in speed or direction, and therefore, the acceleration manifests as a lower frequency content compared to the corresponding velocity and displacement. In other words, this distinction arises from the fact that acceleration, velocity, and displacement are interrelated through the process of differentiation and integration. When the underlying motion involves gradual changes, the resulting acceleration signal may reflect these changes at lower frequencies compared to the corresponding velocity and displacement signals.

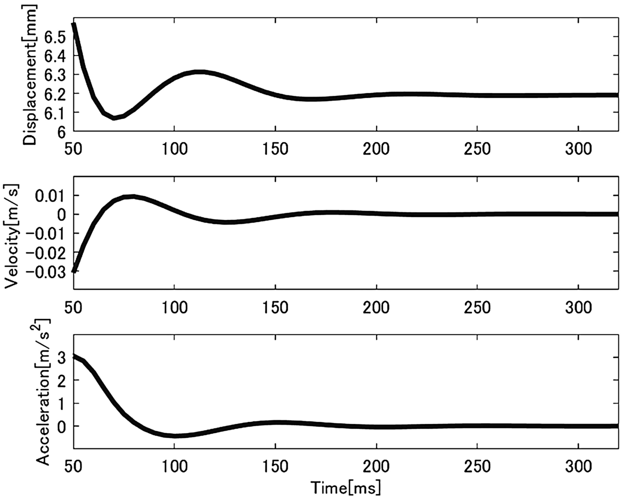

Figure 7 Vertical vibration displacement, velocity, and acceleration graphs based on the FEM simulation

3.2 Derivation method of K and C

For the instantaneous derivation method of K and C, a method of solving a system of equations of motion was used. Here it is assumed that K and C are constant between the current time step ti and the next time step t_{i+1}. As a result, the following system of equations can be created for the current time step and the next time step, as follows:

$$m\ \ddot{z}_i\ + c_i\ \dot{z}_i\ + k_i z_i = 0 \tag{6}$$

$$m\,\ddot{z}_{i+1} + c_i\,\dot{z}_{i+1} + k_i z_{i+1} = 0 \tag{7}$$

where, z, $\dot{z}$, and $\ddot{z}$ respectively denote the relative displacement, velocity, and acceleration of the isolated object, m is the object mass, c is the air layer damping, and k is its stiffness.

The above equation for K and C is as follows:

$$k_i = -\frac{m\,\ddot{z}_{i+1}}{z_{i+1}} - \frac{m\,\dot{z}_{i+1}\left(\ddot{z}_{i+1}\,z_i - \ddot{z}_i\,z_{i+1}\right)}{z_{i+1}\left(\dot{z}_i\,z_{i+1} - \dot{z}_{i+1}\,z_i\right)} \tag{8}$$

$$c_i = \frac{m\left(\ddot{z}_{i+1}\,z_i - \ddot{z}_i\,z_{i+1}\right)}{\dot{z}_i\,z_{i+1} - \dot{z}_{i+1}\,z_i} \tag{9}$$

By using the above equation, instantaneous K and C can be derived at each time step. The derived graph of the time variation of vertical stiffness (K) and vertical damping (C) are shown in Figure 8. It can be seen that K and C are not constant as well as the period, but change from moment to moment.

4 DISCUSSION

This research examined and proposed a formula for the vertical stiffness and damping of air caster systems. Theoretical solutions to the vertical stiffness and damping of such systems were explored. Computer simulations were also conducted to understand the air layer dynamic behavior. It is also concluded that the instantaneous air layer thickness, representing the air chamber pressure, and the bearing inlet flow rate are the key factors in determining the dynamic properties of the air layer. The temporal variation graphs of K and C using the theoretical formula are shown in Figure 9.

Both Figures 8 and 9 illustrate that the air isolator's damping and stiffness are time-dependent values. That means at any specific time, the parameters influencing the air layer stiffness and damping are changing. These influential parameters are, in fact, the pressure of the air below the isolated mass, and the vertical displacement of the mass relative to the ground. The former is mainly related to the air layer stiffness, while the latter represents the air flow outlet section area, which is related to the air layer damping. Therefore, any specific time on these graphs corresponds to a pressure-position binary, which is directly related to the air layer's vertical stiffness and damping. Hence, as long as the boundary conditions and other settings are the same as those used in this paper, the proposed damping and stiffness values would represent the dynamic properties of the isolation system for any specific pressure-position binary (which corresponds to a specific time). In addition, the C and K values in this paper are calculated based on the study of the vertical free vibration of the isolated mass. Therefore, the vertical stiffness and damping presented in Figures 8 and 9 are independent of the type of base excitation. They are valid both for continuous and periodic harmonic excitations, as well as for transient earthquake excitations and those causing temporary disturbances. It should be noted that ultra-high-frequency base excitations are not within the scope of this research. The base excitation frequencies considered in this paper are those falling within the frequencies of earthquake-strong ground motion activities.

It should be noted that this paper has proposed adopting the theoretical concept of air springs and dampers for calculating the stiffness and damping of air seismic isolation systems. However, there is a subtle difference in the mechanism of an air caster and the air damper. An air caster has a clearly separated air inlet and outlet. The air caster puts air into the air layer from the ground or the bottom of the object, and the air exits from the side of the air layer into the atmosphere. On the other hand, the air damper cannot clearly define the gap as the air inlet and the orifice as the air outlet. Moreover, the authors think that it is necessary to consider the formation of a three-dimensional air layer considering the air layer out-of-plane depth, just as when this device is actually used. Accordingly, for the results to be comparable, it is essential to use identical initial and boundary conditions in the two methods. Therefore, the authors believe that although the FEM simulation results presented in section 3 of this paper are valid within the described conditions, a direct comparison of the simulation and theoretical formula graphs requires identical conditions.

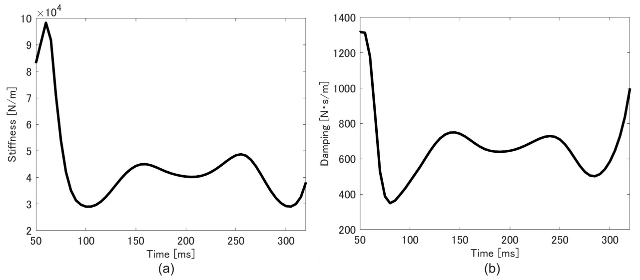

Figure 8 Time history responses of (a) Stiffness, and (b) Damping

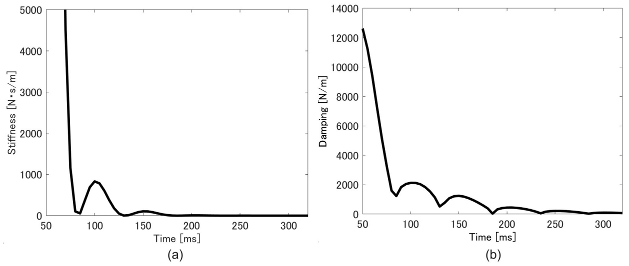

Figure 9 Time history responses of (a) Stiffness, and (b) Damping, based on the theoretical formula

DISCLAIMER

The authors declare no conflict of interest.

ACKNOWLEDGMENTS

This study was supported by the Department of Mechanical Engineering and the Department of Transdisciplinary Science and Engineering, Tokyo Institute of Technology, Tokyo, Japan.

REFERENCES

Adachi, T. and Takahara, K. (2022), 'Development of a semi-active damper vibration control system with a simple structure on a fragile wooden house', *Transactions of the Society of Instrumentation and Control Engineering* **58**(11), 519–526.
URL: *https://doi.org/10.9746/sicetr.58.519*

Aoki, Y., Hiramatsu, A., Wachi, T., Aoki, T., Kajiwara, K. and Tagawa, Y. (2015), 'Development of active seismic base isolation system with mechanical controller', *Transactions of the JSME* **81**(823), 1–14.
URL: *https://doi.org/10.1299/transjsme.15-00230*

AreGo Inc. (2024), 'Air caster technology'. [Accessed 3 April 2024].
URL: *https://www.aerogo.com/products/are-air-casters-right-for-you/*

Asami, T. (1994), 'Utilization of viscous damping', *Noise Control* **18**(3), 120–125.

Bird, J., Santer, M. and Morrison, J. (2018), 'Experimental control of turbulent boundary layers with in-plane travelling waves', *Flow, Turbulence and Combustion* **100**, 1015–1035.
URL: *https://doi.org/10.1007/s10494-018-9910-6*

Fujita, S., Minagawa, K., Tanaka, G. and Shimosaka, H. (2011), 'Intelligent seismic isolation system using air bearings and earthquake early warning', *Soil Dynamics and Earthquake Engineering* **31**, 223–230.
URL: *https://doi.org/10.1016/j.soildyn.2010.04.003*

Furuya, O., Takito, K., Kurabayashi, H., Sampei, K. and Yamazaki, K. (2020), Study on multifunctional base isolation system using air-floating technique, *in* 'ASME Pressure Vessels & Piping Conference'.

Ishiyama, Y. (1992), 'Distribution of seismic layer shear forces and base-shear coefficients for various buildings', *The Architectural Institute of Japan's Journal of Structural and Construction Engineering* **439**.

Ito, M., Sanbonsuga, R., Maeda, M. and Furuno, Y. (2013), Experimental study on seismic performance of reinforced shear walls added to src structures, *in* 'Proceedings of the Annual Meeting of the Concrete Institute', Vol. 35, pp. 379–384.

Kojima, T., Inaba, K. and Takada, Y. (2018), A study for theoretical modeling of cavitation inducement from the solid-fluid interface with fluid-structure interaction, *in* 'ASME Pressure Vessels & Piping Conference', Czech Republic.

Mitsuishi, A., Shimura, T. and Iwamoto, K. (2021), 'Traveling wave control technique for drag reduction of wall turbulence', *The Japan Society of Fluid Mechanics, Nagare* **40**, 271–278.
URL: *https://doi.org/10.5351/nagare.40.271*

Onoda Sngyo Inc. (2024), 'Air caster technology'. [Accessed 20 April 2024].
URL: *https://www.onoda-sg.co.jp/air/*

Sadeghzadeh Nazari, M. and Ghafory Ashtiany, M. (2011), Influential parameters for the design of non-structural components in multi-story buildings, *in* '3rd ECCOMAS Thematic Conference on Computational Methods in Structural Dynamics and Earthquake Engineering, COMPDYN', Greece.

Sadeghzadeh Nazari, M., Numada, M. and Meguro, K. (2015), Introducing a new tuned mass damper system, *in* '7th International Conference of Seismology and Earthquake Engineering, SEE7', Iran.

Sansei Air Danshin System Inc. (2024), 'Air danshin system'. [Accessed 20 April 2024].
URL: *https://airdanshin.co.jp/*

SN-Engineering Inc. (2024), 'Air caster technology'. [Accessed 20 April 2024].
URL: *https://sne-inc.com/aircaster/*

Suwada, H., Fukuyama, H., Mukai, T. and Nomura, S. (2005), Structural testing of high-performance earthquake-resistant elements that combine strength, rigidity, and toughness, *in* 'Proceedings of the Annual Meeting of the Concrete Institute', Vol. 27, pp. 1087–1092.

Xu, P., Inaba, K., Takeishi, H. and Kagawa, T. (2023), Feasibility and optimization of nozzle flapper system for position measurements of high-speed rotation spindle with aerostatic bearings, *in* 'ASME Pressure Vessels & Piping Conference', USA.

You, J. H. and Inaba, K. (2013), 'Fluid–structure interaction in water-filled thin pipes of anisotropic composite materials', *Fluids and Structures* **36**, 162–173.
URL: *https://doi.org/10.1016/j.jfluidstructs.2012.07.009*

[This page is intentionally left blank]